

# A Simple Review of EEG Foundation Models: Datasets, Advancements and Future Perspectives

Junhong Lai<sup>1,2,3</sup>, Jiyu Wei<sup>1,2,3</sup>, Lin Yao<sup>1,2,3</sup> and Yueming Wang<sup>1,2,3,4</sup>

<sup>1</sup>The College of Computer Science, Zhejiang University, Hangzhou, China.

<sup>2</sup>The MOE Frontiers Science Center for Brain and Brain-Machine Integration, Zhejiang University, Hangzhou, China.

<sup>3</sup>The Nanhu Brain-Computer Interface Institute, Hangzhou, China.

<sup>4</sup>The Qiushi Academy for Advanced Studies, Hangzhou, China.

**Electroencephalogram (EEG) signals play a crucial role in understanding brain activity and diagnosing neurological disorders. This review focuses on the recent development of EEG foundation models(EEG-FMs), which have shown great potential in processing and analyzing EEG data. We discuss various EEG-FMs, including their architectures, pre-training strategies, their pre-training and downstream datasets and other details. The review also highlights the challenges and future directions in this field, aiming to provide a comprehensive overview for researchers and practitioners interested in EEG analysis and related EEG-FMs.**

**Index Terms**—Electroencephalogram (EEG), EEG foundation model(EEG-FM).

## I. INTRODUCTION

**E**EG is a non-invasive technique that records the electrical activity of the brain. It has been widely used in neuroscience research, clinical diagnosis, and brain-computer interfaces (BCIs) [1]. However, EEG data analysis is challenging due to its low signal-to-noise ratio (SNR), high dimensionality, non-stationarity, and individual variability [2], [3]. As highly objective physiological signals, EEG has demonstrated remarkable potential in seizure epilepsy classification [4], acute stress detection [5], sleep stage classification [6], motor imagery recognition [7], abnormal identification [8], emotion analysis [9], and auditory attention detection [10].

Although EEG modeling has attracted extensive research attention, several issues remain unresolved. Currently, research on EEG recording modeling is mainly divided into two research lines, including manual feature methods [11] and deep learning-based methods [12]. Manual feature engineering requires a lot of domain knowledge and may only be applicable to specific tasks. In addition, most deep learning-based methods are fully supervised, which heavily relies on labeled data. However, large-scale labeled data is often infeasible or expensive in medical experiments, highlighting the importance of maximizing labeling efficiency.

In recent years, the emergence of large-scale pre-training models has revolutionized the field of natural language processing(LLM) [13], [14] and computer vision(VLM) [15]–

[17]. Inspired by these successes, researchers have started to explore the application of large models in EEG analysis [18]. These models can learn hierarchical representations from large amounts of unlabeled EEG data, which can then be fine-tuned for specific tasks, such as seizure detection, emotion recognition, and cognitive state assessment. This approach has the potential to improve the performance and generalization ability of EEG analysis models, while reducing the need for labeled data [19].

Motivated by the potential of EEG-FMs(EEG Foundation Models) and an increasing number of recent papers proposing EEG-FMs for various EEG tasks, there is an urgent need for a comprehensive review of EEG-FMs for EEG applications. The main contributions of this paper include:

- Summarizing the overview of different EEG-FMs.
- Summarizing the datasets for pre-training and downstream of EEG-FMs.
- Summarizing the details for pre-training and evaluation of EEG-FMs.
- Future perspectives for EEG-FMs.

By addressing these essential aspects, this review paper will provide a comprehensive and in-depth analysis of the application of EEG-FMs for EEG tasks. The goal of this review is to provide a comprehensive overview of the current state-of-the-art EEG foundation models. The models we investigated include the following: Brant [19]<sup>1</sup>, BrainWave(Brant-2) [20]<sup>2</sup>, LaBraM [21]<sup>3</sup>, NeuroGPT [22]<sup>4</sup>, BIOT [23]<sup>5</sup>, EEGPT1 [24]<sup>6</sup>, BrainBERT [25]<sup>7</sup>, FoME [26]<sup>8</sup>, EEGPT2 [27], MBrain [28], NeuroLM [29], CBraMod [30]<sup>9</sup> and EEGFormer [31].

We will discuss the key techniques and architectures used in these models, their performance on various tasks, and the challenges and future directions in this field. By summarizing the latest research findings, we hope to promote further research

<sup>1</sup>Github: <https://zju-brainnet.github.io/Brant.github.io/>

<sup>2</sup>Github: <https://github.com/yzz673/Brant-2>

<sup>3</sup>Github: <https://github.com/935963004/LaBraM>

<sup>4</sup>Github: <https://github.com/wenhui0206/NeuroGPT>

<sup>5</sup>Github: <https://github.com/ycq091044/BIOT>

<sup>6</sup>Github: <https://github.com/BINE022/EEGPT>

<sup>7</sup>Github: <https://github.com/czlwang/BrainBERT>

<sup>8</sup>Github: <https://github.com/1061413241/FoME>

<sup>9</sup>Github: <https://github.com/wjq-learning/CBraMod>

and development in EEG foundation models and facilitate their application in clinical and research settings.

## II. OVERVIEW OF EEG FOUNDATION MODELS

EEG-FMs have emerged as a powerful tool in the analysis and interpretation of EEG signals, leveraging large-scale data and unsupervised training approaches, similar to other large models like those used in NLP fields. These models aim to capture complex temporal and spatial dependencies in EEG data, which can be utilized for tasks such as classification, prediction, and anomaly detection. EEG-FMs have gained significant attention due to their ability to model intricate patterns in brain activity, with applications in clinical diagnostics, cognitive neuroscience, BCIs, and more. EEG-FMs typically undergo unsupervised pretraining using vast datasets, allowing the model to learn relevant features and representations from EEG signals without the need for extensive labeled data.

In EEG-related tasks, the input consists of multichannel EEG recordings, where each channel corresponds to a node, and the connectivity between channels (based on functional or structural relationships) represents edges in the model. The data is typically time-series, meaning each EEG signal consists of a series of voltage readings sampled over time, often captured from multiple electrodes placed on the scalp. A large model learns to extract patterns from these signals, and the objective is to predict or classify brain states, such as detecting epileptic seizures, identifying cognitive states, or differentiating between disorders like ADHD or Alzheimer’s disease.

Compared to traditional machine learning models, EEG-FMs offer several advantages. First, like other large models, they are capable of learning representations directly from raw EEG data, which bypasses the need for manual feature extraction. This ability to handle complex, high-dimensional data makes them particularly powerful for EEG analysis, as they can learn both temporal and spatial patterns from the raw signal. EEG-FMs are also designed to handle the large-scale and diverse nature of EEG data, which may come from different subjects, tasks, and experimental conditions, making them highly versatile and robust. Furthermore, similar to other deep learning models, EEG-FMs can learn hierarchical representations, capturing both low-level features (e.g., oscillatory patterns) and high-level brain network dynamics, leading to improved performance on a variety of tasks. Several advanced techniques in EEG-FMs, such as transformers and self-supervised learning, allow the model to leverage vast amounts of unlabelled EEG data for pretraining, significantly improving generalization to new, unseen data.

The architecture of EEG-FMs varies depending on the task, but common approaches mainly include convolutional neural networks (CNNs) and transformers. These models are typically designed to process the temporal aspect of EEG signals (e.g., using CNNs) as well as the spatial relationships between electrodes (e.g., using attention mechanisms). In particular, transformer models, which have been successful in natural language processing, have been adapted to handle EEG data by processing long-term temporal dependencies and capturing

complex spatial relationships between EEG channels. The large-scale nature of EEG-FMs enables them to generalize across different subjects and experimental conditions, making them suitable for a wide range of applications, including brain-computer interfaces (BCIs), cognitive state monitoring, and clinical diagnostics.

EEG-FMs are trained on vast amounts of EEG data from multiple sources, ensuring that the model learns the underlying patterns that are consistent across different individuals and experimental conditions. By using unsupervised learning techniques, such as contrastive learning or self-supervised learning, EEG-FMs can efficiently learn from large datasets without requiring manual labeling, which is often a significant challenge in EEG research. The ability to scale up to large datasets also allows EEG-FMs to adapt to diverse applications, from medical diagnosis to real-time brain-state monitoring in brain-computer interfaces.

The key benefits of EEG-FMs over traditional deep learning approaches are their ability to handle large-scale, multichannel, and high-dimensional time-series data, as well as their capacity to generalize across different subjects and conditions. Like other large models, they are designed to scale with increasing data and computational resources, making them ideal for tasks requiring sophisticated understanding of brain activity. The challenge, however, lies in the computational demands of training such large models, which require significant GPU resources and sophisticated optimization techniques to ensure efficient learning. Additionally, there are ongoing efforts to improve model interpretability and avoid issues such as overfitting, where the model may fail to generalize to new or unseen EEG data. Recent advancements in techniques such as attention mechanisms and hybrid models that combine temporal and spatial processing are helping to address these challenges, further enhancing the potential of EEG-FMs.

### A. Data collection and preprocessing

Large language model pretraining usually requires a lot of data, and so does the EEG foundation model. Therefore, the first step in pretraining a large model is usually to collect as many EEG datasets as possible to ensure that the diversity and representativeness of the pretraining dataset can fully ensure that the model can fully learn the various characteristics of brain activity.

EEG data usually has a low SNR, and the preprocessing of the data usually includes: bandpass filtering, notch filtering, resampling and normalization. Generally speaking, there is no need to use ICA for additional artifact removal. We discuss the preprocessing steps of each EEG-FM in detail in Section.III-B.

- **Bandpass filtering.** Bandpass filter the EEG signal to remove low-frequency noise (e.g. 0.1 Hz - 75 Hz).
- **Notch filtering.** Apply a notch filter to avoid power line interference (e.g. 50 Hz).
- **Resampling.** Resample all EEG signals (e.g. 200hz).
- **Normalization.** Normalize the EEG signal (e.g., z-score).

### B. Model architecture

In this section, we detail the whole framework of universal EEG-FM, though their model architecture details and pre-

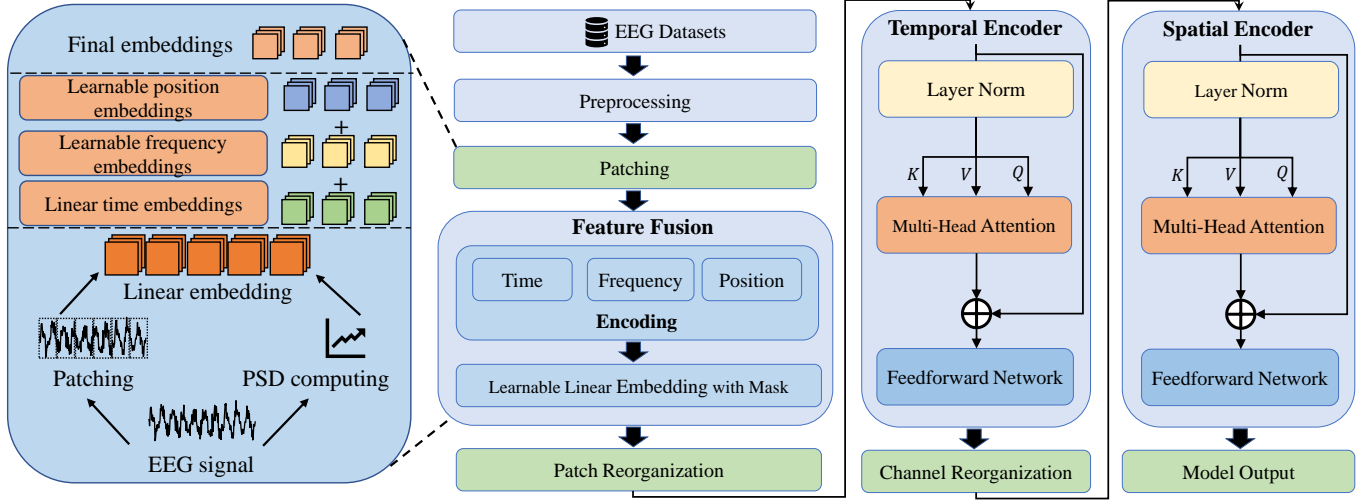


Fig. 1: Overview of the architecture and workflow of general EEG-FM.

training details may not be exactly the same. The Overview of the architecture and workflow of general EEG-FM is illustrated in Fig.1. We can formulate the multi-channel EEG signals as  $\mathbf{X} \in \mathbb{R}^{T \times C}$ , where  $C$  is the number of EEG channels and  $T$  is the total timestamps.

### 1) Patching

Since neural recordings are electrical signals with high sampling rates, we aggregate timestamps into patches to (1) enhance the locality and extract semantic information; (2) reduce computation and memory usage; and (3) attend a longer temporal dependency [32]. Assume that the timestamp for each sample is  $t$  and the stride is  $s$ .  $X$  can be segmented into  $\lfloor \frac{T-t}{s} + 1 \rfloor$ , and each sample  $x \in \mathbb{R}^{t \times C}$ , where  $t$  is the number of timestamps and  $C$  is the number of electrode channels, we divide  $x$  with length  $M$ , stride  $S$  and overlap  $O$ , where  $O = M - S$  is the number of overlapping timestamps between consecutive patches. This generate a set of patches  $\mathbf{p} \in \mathbb{R}^{N_p \times C \times M}$ , where  $N_p = \lfloor \frac{t-M}{S} + 1 \rfloor$  is the number of patches in each channel. In fact,  $\mathbf{p}$  can be represent as:

$$\left\{ \mathbf{p}_{k,c} \in \mathbb{R}^M \mid k = 1, 2, \dots, \left\lfloor \frac{t-M}{S} + 1 \right\rfloor; c = 1, 2, \dots, C \right\} \quad (1)$$

### 2) Time-Encoding

The time-encoding is composed of a linear projection layer. Specifically, the input  $\mathbf{p} \in \mathbb{R}^{N_p \times C \times M}$  contains  $N_p \times C$  patches with length  $M$  and  $\mathbf{p}_c \in \mathbb{R}^{N_p \times M}$  denotes the patches in  $c$ -th channel. We map each sequence of patches  $\mathbf{p}_c \in \mathbb{R}^{N_p \times M}$  to the latent space of dimension  $D$  by a linear projection  $\mathbf{W}_{proj} \in \mathbb{R}^{M \times D}$ , which can be presented as  $e_c = (\mathbf{W}_{proj}^T \mathbf{p}_c)^T$ . We denote the time-encoding embeddings as  $e \in \mathbb{R}^{N_p \times C \times D}$ :

### 3) Frequency-Encoding

The frequency-encoding mainly extracts the power density value corresponding to each frequency and calculated the power sum within the frequency band according to the preset  $n$  frequency band intervals  $[f_{min}, f_{max}]$ , where  $0 < f_{min} < f_{max} < f_{Nyquist}$  [33]. For EEG signals, we usually divide the

frequency spectrum into five bands:  $\delta$  (1-4Hz),  $\theta$  (48Hz),  $\alpha$  (8-13Hz),  $\beta$  (13-30Hz),  $\gamma$  (30-50Hz). For the  $i$ -th frequency band, a learnable encoding  $\mathbf{f}_i \in \mathbb{R}^{N_p \times D}$  is set as its representation which is shared across all the patches. For a given patch  $P_{k,c}(t) = p_{k,c}$ , we first apply the Fourier transform [34] to convert the time-domain signal into the frequency domain. The power spectral density(PSD), denoted as  $P_{k,c}(f)$ , is then calculated by squaring the magnitude of the frequency components:

$$P_{k,c}(f) = \frac{1}{T} |\mathcal{F}\{P_{k,c}(t)\}|^2 = \frac{1}{T} \left| \int_{-\infty}^{\infty} P_{k,c}(t) e^{-i2\pi f t} dt \right|^2 \quad (2)$$

where  $f$  is the frequency,  $T$  is the total duration of the signal segment, and  $\mathcal{F}$  is the Fourier transform. Subsequently, we compute the sum of power within each sub-band  $[f_{min}, f_{max}]$ :

$$PSD_{k,c}(i) = \log_{10} \left( \sum_{f_i=f_{min}}^{f_{max}} P_{k,c}(f) + 1 \right) \quad (3)$$

$PSD_{k,c}(i)$  acts as the weight of  $\mathbf{f}_i$ . The frequency encoding  $\mathbf{F}_{k,c} \in \mathbb{R}^D$  of patch  $p_{k,c}$  is obtained as the weighted sum of the learnable encodings  $\mathbf{f}_i$ :

$$\mathbf{F}_{k,c} = \sum_{i=1}^{|\text{bands}|} \frac{\exp(P_{k,c}(i))}{\sum_{i'=1}^{|\text{bands}|} \exp(P_{k,c}(i'))} \mathbf{f}_i \quad (4)$$

### 4) Position-Encoding

A learnable positional encoding  $\mathbf{W}_{c,pos} \in \mathbb{R}^{N_p \times D}$  monitors the temporal order of patches  $\mathbf{p}_c \in \mathbb{R}^{N_p \times M}$ .

### 5) Time-Frequency Fusion

According to the previous steps, we can obtain the time-encoding  $e \in \mathbb{R}^{N_p \times C \times D}$ , frequency-encoding  $\mathbf{F} \in \mathbb{R}^{N_p \times C \times D}$ , position-encoding  $\mathbf{W}_{pos} \in \mathbb{R}^{N_p \times C \times D}$ . We can obtain the fusion-encoding  $\tilde{\mathbf{p}} \in \mathbb{R}^{N_p \times C \times D}$  by adding them together:

$$\tilde{\mathbf{p}} = e + \mathbf{F} + \mathbf{W}_{pos} \quad (5)$$

### 6) Temporal Encoder

The Temporal Encoder is designed to capture long-range dependencies and intricate temporal patterns within EEG data, which consists of a stack of dense Transformer encoding layers. Each layer encompasses three key modules: multi-head self-attention, feedforward neural network, and layer normalization with residual connections. Given an input embedding  $\tilde{\mathbf{p}} \in \mathbb{R}^{N_p \times C \times D}$  obtained from the previous step, we apply a trainable linear transformation along the temporal dimension to derive the query, key, and value matrices for the attention operation, denoted as  $\mathbf{Q}_{time}^i, \mathbf{K}_{time}^i, \mathbf{V}_{time}^i \in \mathbb{R}^{N_p \times D}$  respectively. The temporal dependencies are then modeled by computing the attention score  $\text{Attention}_{time}^i$ :

$$\text{Attention}_{time}^i = \text{Softmax}(\mathbf{Q}_{time}^i (\mathbf{K}_{time}^i)^T / \sqrt{D}) \mathbf{V}_{time}^i \quad (6)$$

In the multi-head self-attention mechanism, the query, key, and value matrices are linearly projected into  $D_k, D_k, D_v$ . Subsequently, the attention function is applied to each projected version, yielding an output of dimension  $D_v$ . These outputs are concatenated and mapped back to the original dimension  $D$  to obtain the final attention value:

$$\text{MultiHead}(Q, K, V) = \text{Concat}(\text{head}_1, \dots, \text{head}_h) W^O \quad (7)$$

where  $\text{head}_i = \text{Attention}(\mathbf{Q} W_i^Q, \mathbf{K} W_i^K, \mathbf{V} W_i^V), W_i^Q \in \mathbb{R}^{D \times D_k}, W_i^K \in \mathbb{R}^{D \times D_k}, W_i^V \in \mathbb{R}^{D \times D_v}$ , and  $W^O \in \mathbb{R}^{D \times h D_v}$  denote the projection matrix. Finally get the output  $\hat{\mathbf{p}} \in \mathbb{R}^{N_p \times C \times D}$ .

### 7) Spatial Encoder

The Spatial Encoder is specifically designed to capture spatial relationships and inter-channel dynamics within EEG data. Recognizing the intricate interactions between different brain regions represented by distinct EEG channels, this encoder adapts to learn channel-specific characteristics and their interdependencies. Similarly, given an input embedding  $\hat{\mathbf{p}} \in \mathbb{R}^{N_p \times C \times D}$  obtained from the previous step, we apply a trainable linear transformation along the channel dimension to derive the query, key, and value matrices for the attention operation, denoted as  $\mathbf{Q}_{ch}^i, \mathbf{K}_{ch}^i, \mathbf{V}_{ch}^i \in \mathbb{R}^{N_p \times D}$  respectively. Finally, we compute the attention score  $\text{Attention}_{ch}^i$ , which involves the interactions between channels and represents the spatial dynamics of the brain:

$$\text{Attention}_{ch}^i = \text{Softmax}(\mathbf{Q}_{ch}^i (\mathbf{K}_{ch}^i)^T / \sqrt{D}) \mathbf{V}_{ch}^i \quad (8)$$

The application of multi-head self-attention mechanism in this part is similar to the previous part. Finally get the output  $\bar{\mathbf{p}} \in \mathbb{R}^{N_p \times C \times D}$ .

### C. Reconstruction

Constructing the reconstruction loss allows the model to learn the potential representation of EEG data and the spatio-temporal and frequency domain characteristics of EEG data on unlabeled data through self-supervised learning tasks, thereby improving the model's adaptability to noise and occlusion.

The overview of neural tokenizer training and EEG-FM pre-training is illustrated in Fig.2.

The existing model mainly includes the following four types of reconstruction objectives(see Tab.VII): original patches, potential representation of patches(embeddings), frequency domain features of patches, and codebook prediction.

#### 1) Reconstruction of original patches

During the pre-training stage, the representations  $\bar{\mathbf{p}} \in \mathbb{R}^{N_p \times C \times D}$  will be fed into a flatten layer with linear head  $W_{rec} \in \mathbb{R}^{D \times M}$  to reconstruct the original patches  $\check{\mathbf{p}} \in \mathbb{R}^{N_p \times C \times M}$ . Finally we utilize an MSE loss to measure the discrepancy between the reconstructed patches and the original patches:

$$\mathcal{L}_{op} = \frac{1}{N_p} \sum_i^{N_p} \|\mathbf{p}_i - \check{\mathbf{p}}_i\|_2^2 \quad (9)$$

where  $\check{\mathbf{p}}_i, \mathbf{p}_i \in \mathbb{R}^{C \times M}, i = 1, 2, \dots, N_p$ .

#### 2) Reconstruction of patches embeddings

We utilize an MSE loss to measure the discrepancy between the reconstructed patches embeddings  $\tilde{\mathbf{e}} \in \mathbb{R}^{N_p \times C \times D}$  and the patches embeddings  $\tilde{\mathbf{p}} \in \mathbb{R}^{N_p \times C \times D}$ :

$$\mathcal{L}_{pe} = \frac{1}{N_p} \sum_i^{N_p} \|\tilde{\mathbf{e}}_i - \tilde{\mathbf{p}}_i\|_2^2 \quad (10)$$

where  $\tilde{\mathbf{p}}_i, \tilde{\mathbf{e}}_i \in \mathbb{R}^{C \times D}, i = 1, 2, \dots, N_p$ .

#### 3) Reconstruction of fourier spectrum

For an EEG patch  $p_{k,c} = [p[1], p[2], \dots, p[N_p]]$  of channel  $c$  and time  $k$  in a sample  $p$ , we apply the Discrete Fourier Transform (DFT) as follows:

$$\tilde{p}_{c,k}^m = \sum_{n=1}^{N_p} p[n] \exp\left(-\frac{2\pi j}{N_p} mn\right) \quad (11)$$

where  $m \in [1, N_p]$  and  $j$  is the imaginary unit. We rewrite Equation 11 using Euler's formula as:

$$\tilde{p}_{c,k}^m = \sum_{n=1}^{N_p} p[n] \cos\left(\frac{2\pi}{N_p} mn\right) - jp[n] \sin\left(\frac{2\pi}{N_p} mn\right) \quad (12)$$

where  $\tilde{p}_{c,k}^m$  indicates the spectrum of the sequence at frequency  $\omega_m = \frac{2\pi m}{N_p}$ . The amplitude and phase can be calculated as:

$$\begin{cases} A^m = \sqrt{\text{Re}(\tilde{p}_{c,k}^m)^2 + \text{Im}(\tilde{p}_{c,k}^m)^2} \\ \phi^m = \arctan\left(\frac{\text{Im}(\tilde{p}_{c,k}^m)}{\text{Re}(\tilde{p}_{c,k}^m)}\right) \end{cases} \quad (13)$$

where  $Re$  and  $Im$  represent the real and imaginary parts of a complex number. We usually apply z-score normalization to normalize  $A^m$  and  $\phi^m$  within a sample for stable convergence.

The output representations are aggregated by average pooling followed by two specific prediction heads to regress the spectrum amplitude  $o^A$  and phase  $o^\phi$ , respectively. The mean squared error (MSE) loss is utilized to guide the prediction:

$$\mathcal{L}_A = \frac{1}{N_p} \sum_{i=1}^{N_p} \|o_i^\phi - \phi_i\|_2^2 \quad (14)$$

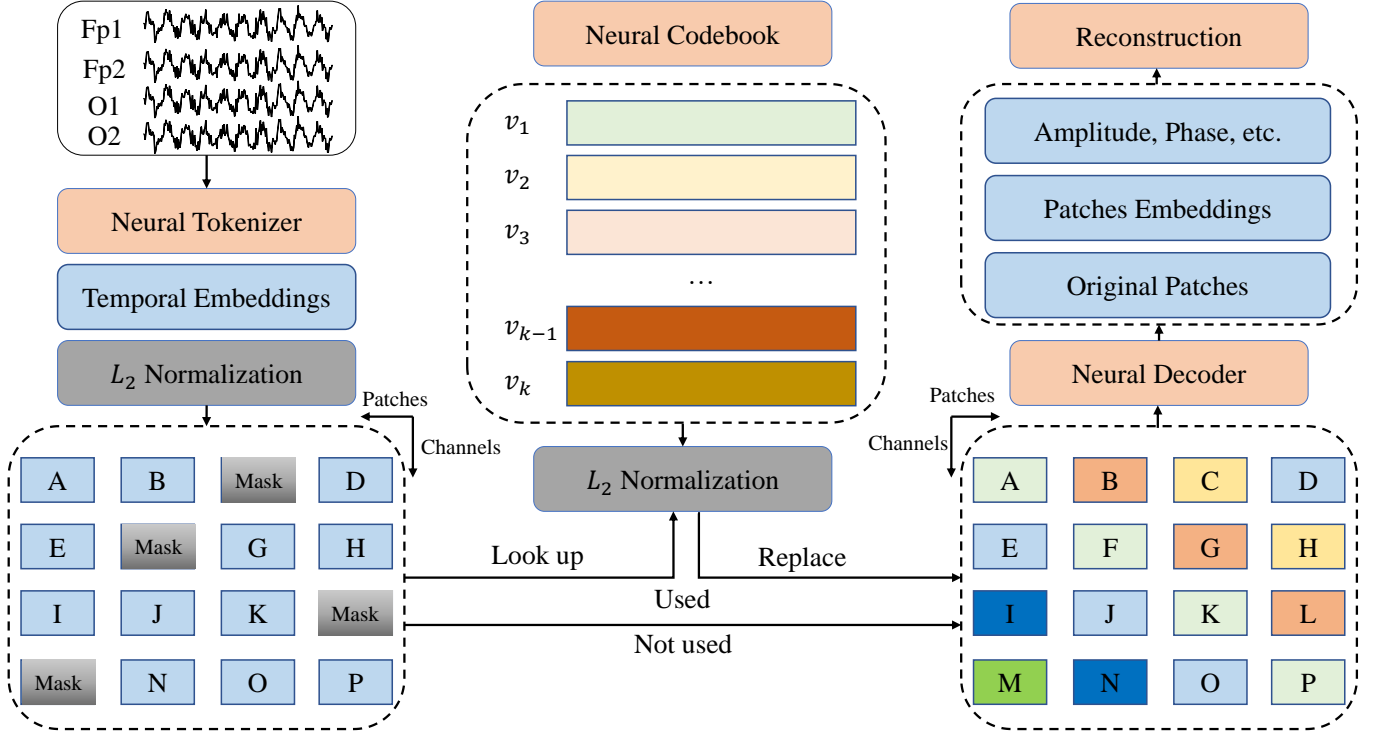


Fig. 2: Overview of neural tokenizer training and EEG-FM pre-training.

$$\mathcal{L}_\phi = \frac{1}{N_p} \sum_{i=1}^{N_p} \|o_i^\phi - \phi_i\|_2^2 \quad (15)$$

#### 4) Codebook prediction

Codebook prediction consists of two parts: Neural tokenizer training and embedding prediction.

For **Neural Tokenizer Training**: We define a neural codebook  $\mathcal{V} = \{v_i | i = 1, \dots, K\} \in \mathbb{R}^{K \times D}$ , where  $K$  is the number of the discrete neural embeddings and  $D$  is the dimensionality of each embedding. All time-encoding embeddings  $e \in \mathbb{R}^{N_p \times C \times D}$  are stored in the codebook  $\mathcal{V}$ . We utilize a quantizer to quantize all the patch representations into the neural codebook embeddings. The codebook looks up the nearest neighbor of each patch  $p_i$  in the neural codebook  $\mathcal{V}$ . This procedure can be formulated as:

$$z_i = \arg \min_j \|\ell_2(p_i) - \ell_2(v_j)\|_2, \quad (16)$$

where  $\ell_2$  represents  $\ell_2$  normalization and  $z_i$  is the quantized vector after the quantizer. This is equivalent to finding the closest neural embedding by cosine similarity and such  $\ell_2$  normalization improves the codebook utilization [35].

$$\mathcal{L}_{ntt} = \frac{1}{N_p} \sum_i^{N_p} \|\mathbf{sg}(\ell_2(p_i)) - \ell_2(v_{z_i})\|_2^2 + \|\ell_2(p_i) - \mathbf{sg}(\ell_2(v_{z_i}))\|_2^2 \quad (17)$$

where  $sg$  represents the stop-gradient operation that is defined as an identity at the forward pass and has zero gradients.

For **Embedding prediction**: We randomly generate a mask  $\mathcal{M} = \{m_i \in \{0, 1\} | i = 1, \dots, N_p\}$ . After that, we replace the masked patches of  $p$  with the learnable

mask token  $e_{\mathcal{M}} \in \mathbb{R}^D$ . The corrupted EEG patches can be denoted as  $e^{\mathcal{M}} = \{e_i : m_i = 0 | i = 1, 2, \dots, N_p\} \cup \{e_{\mathcal{M}} : m_i = 1 | i = 1, 2, \dots, N_p\}$ , which will be added by subsequent modules.  $\bar{p} \in \mathbb{R}^{N_p \times C \times D}$  are used to predict the corresponding neural tokens through a linear classifier:

$$p(v' | e^{\mathcal{M}}) = \text{softmax}(\text{Linear}(\bar{p})) \quad (18)$$

The linear layer outputs a vector  $o_i \in \mathbb{R}^{\mathcal{V}}$  of length  $\mathcal{V}$ , where each element  $o_{i,j}$  represents the unnormalized probability that the patch is predicted to be the  $j$ -th token in the Codebook. The Softmax function converts the unnormalized probability into a probability distribution.

$$p(v'_j | e^{\mathcal{M}}) = \frac{\exp(o_{i,j})}{\sum_{k=1}^{\mathcal{V}} \exp(o_{i,k})}, \quad j = 1, 2, \dots, \mathcal{V} \quad (19)$$

where  $p(v' | e^{\mathcal{M}})$  is the probability that the model predicts that the token corresponding to  $\bar{p}_i$  is  $v_j$ .

The objective training loss is:

$$\mathcal{L}_{eq} = - \sum_{m_i=1} \log p(v_i | e^{\mathcal{M}}) \quad (20)$$

### III. SURVEY RESULTS

This survey is based on a review of 11 articles. These articles were selected by title and abstract screening from a search on Google Scholar and ScienceDirect queried on December 9st, 2024. The search query for collecting the articles was defined as: (“LLM” OR “Foundation model”)

AND (“Electroencephalography” OR “EEG”). Both peer-reviewed articles and preprints were included. All types of EEG foundation model were included.

In the remaining portion of this paper, we report the categories of comparisons we identified in the surveyed papers. These are based on the different aspects of the proposed EEG-based LMs. Specifically, these are:

- Datasets for pretraining and downstream tasks.
- Preprocessing conditions of datasets.
- The evaluation methods of EEG-FMs.
- The parameter size of EEG-FMs.
- The objective loss function of EEG-FMs.
- The hardware conditions for pre-training of EEG-FMs.

The following parts will provide further details on these aspects, and the paper will conclude by discussing trends and proposing plausible directions for future research.

#### A. Pretraining and Downstream Datasets

In the pre-training of EEG foundation models, the diversity and representativeness of dataset are crucial. In order to ensure that the model can fully learn the various characteristics of brain activity, a large amount of EEG signal data must be collected. For research teams with conditions, these data not only include public data sets, but can also be combined with self-collected data. Comprehensive data collection usually needs to take into account task diversity, subject diversity, diversity of collection conditions, and diversity of time spans and frequencies. Through comprehensive and diverse data collection, EEG foundation models can obtain richer training data, and then learn more universal and detailed features, thereby demonstrating better performance and generalization capabilities in practical applications. According to our statistics(see Tab.I), Brant-2 uses the most pre-training data, reaching 13.79TB, and the EEG recording time is about 40,000 hours.

TABLE I: The size and length of EEG datasets used to pre-train the model

Model	Size	Length
Brant [19]	1.01TB	2528h
Brant-2 [20]	13.79TB	40,907h
LaBraM [21]	-	about 2,500h
NeuroGPT [22]	-	5656h
BIOT [23]	-	-
EEGPT1 [24]	-	-
BrainBERT [25]	-	43.7h
FoME [26]	1.7TB	about 26,000h
EEGPT2 [27]	-	-
MBrain [28]	at least 550GB	at least 470h
NeuroLM [29]	-	about 25,000h
CBraMod [30]	-	27,062h
EEGFormer [31]	1.7TB	about 26,000h

- Indicates that the corresponding article does not explicitly mention the size or length of EEG datasets for pre-training.

In addition, to evaluate the performance of EEG foundation models in downstream tasks, it is necessary not only to use standard performance indicators, but also to pay attention to the model’s generalization ability, interpretability, robustness, computational efficiency and other dimensions. Therefore, the

selection of downstream task data also needs to take into account the relevance and complexity of the task. We have collected all relevant datasets for pre-training and downstream tasks for all the models, see the Tab.II and Tab.III .

TABLE II: Datasets for pretraining and downstream tasks

	Pretraining Datasets	Downstream Datasets
Brant [19]	**	MAYO [36]
	-	FNUSA [36]
	-	**
	CCEP [37]	AD-65 [38]
	CAP [39]	CHB-MIT [40]
	HMS [41]	Mayo-Clinic [36]
	Siena [42]	FNUSA [36]
	SRM [43]	MDD-64 [44]
	TUEG [45]	Depression-122 [46]
Brant-2 [20]	Schizophrenia-81	Schizophrenia-28 [47]
	Sleep-EDF [48]	ADHD-Adult [49]
	Stroke-50 [50]	ADHD-Child [51]
	PD-31 [52]	SD-71 [53]
	IowaDataset	-
	UNMDataset	-
	AD-184 [54]	-
	**	-
	BCICIV-1 [55]	TUAB [56]
	Emobrain [57]	TUEV [56]
	Grasp and Lift [58]	SEED-V [59]
	Inria BCI [60]	MoBI [61]
	MMI [62]	-
	RAW [63]	-
	RSEEG [64]	-
LaBraM [21]	Siena [42]	-
	TVNT [65]	-
	TUAR [66]	-
	TUEP [67]	-
	TUSZ [56]	-
	TUSL [68]	-
	SEED [69]	-
	SEED-V [59]	-
	SEED-GER [70]	-
	Self-collected [71]-[75]	-
NeuroGPT [22]	TUH [56]	BCIC-2A [76]
	SHHS [77], [78]	-
	PREST(*)	-
	Cardiology [79]	-
	CHB-MIT [40]	-
BIOT [23]	IIIC-Seizure [80]	-
	TUAB [56]	-
	TUEV [56]	-
	PTBXL [81]	-
	HAR [82]	-
	PhysioMI [83]	BCIC-2A [76]
	HGD [84]	BCIC-2B [85]
	TSU [86]	Sleep-EDF <sub>x</sub> [48]
EEGPT1 [24]	SEED [69]	KaggleERN [60]
	M3CV [87]	PhysioP300 [83]
	-	TUAB [56]
	-	TUEV [56]

\*\* Indicates the dataset may be private and the authors have not explicitly cited any literature in the paper.

\* Indicates the corresponding dataset is private .

The data not cited any literature in the table are not mentioned in the corresponding article.

#### B. Datasets preprocessing

In the data preprocessing of EEG signals, denoising, artifact removal and standardization are generally required. If you consider using EEG signals as pre-training data, you generally need to resample all EEG signals to a certain frequency (such

TABLE III: Datasets for pretraining and downstream tasks(continued)

	Pretraining Datasets	Downstream Datasets
BrainBERT [25]	-	-
FoME [26]	TUEG [45]	TUEV [56]
	SEED [69]	SEED [69]
	SEED-IV [70]	SEED-IV [70]
	CHB-MIT [40]	CHB-MIT [40]
	Sleep-EDFx [48]	Sleep-EDFx [48]
	MI-Dataset [62]	MAYO [36]
	MAYO [36]	FNUSA [36]
EEGPT2 [27]	FNUSA [36]	-
	FACED [88]	FACED [88]
	SEED [69]	DEAP [89]
	SEED-FRA [90]	SEED-IV [70]
	SEED-GER [70]	SEED-V [59]
	SEED-IV [70]	MIBCI [91]
	SEED-V [59]	BCIC4-1 [55]
	THINGS-EEG-10Hz [92]	EEGMat [93]
	THINGS-EEG-5Hz [94]	EDF [48]
	IMG(*)	HMC [95]
	-	IMG(*)
	-	SPE [96]
	-	DREAMER [97]
	MBrain [28]	SEEG(*)
TUSZ [56]		TUSZ [56]
NeuroLM [29]	TUEG [45]	-
	SEED [69]	TUAB [56]
	SEED-FRA [90]	TUEV [56]
	SEED-GER [70]	SEED [69]
	SEED-IV [70]	HMC [95]
	SEED-V [59]	EEGMat [93]
	BCIC4-1 [55]	TUSL [68]
	Emobrain [57]	-
	Grasp and Lift [58]	-
	MMI [62]	-
	RAW [63]	-
	RSEEG [64]	-
	Siena [42]	-
	SPIS [98]	-
TVNT [65]	-	
**	-	
CBraMod [30]	TUEG [45]	FACED [88]
	-	SEED-V [59]
	-	PhysioMI [83]
	-	SHU-MI [83]
	-	ISRUC [99]
	-	CHB-MIT [40]
	-	BCIC2020-3 [100]
	-	MDD-64 [44]
	-	SEED-VIG [101]
	-	EEGMat [93]
EEGFormer [31]	TUEG [45]	TUAB [56]
	-	TUAB [66]
	-	TUSL [68]
	-	TUSZ [56]
	-	Neonate [102]

\*\* Indicates the dataset may be private and the authors have not explicitly cited any literature in the paper.

\* Indicates the corresponding dataset is private .

The data not cited any literature in the table are not mentioned in the corresponding article.

as 256hz) and then filter (for example, using filters to remove low-frequency, high-frequency and power noise, such as 0.1Hz and 100Hz bandpass filters and 50Hz notch filters) and then standardize. This process helps to unify the data format and reduce data inconsistency, so that the model can learn features from it more effectively. We have counted the preprocessing

of EEG signals for all models, see the Tab.IV.

TABLE IV: The preprocessing conditions of EEG datasets

Model	Resample	Filtering	Standardize
Brant [19]	✓, 250Hz	×	×
Brant-2 [20]	✓	✓	×
LaBraM [21]	✓, 200Hz	✓	✓
NeuroGPT [22]	✓, 250Hz	✓	✓
BIOT [23]	✓	×	✓
EEGPT1 [24]	✓, 256Hz	✓	✓
BrainBERT [25]	✓	✓	✓
FoME [26]	✓, 250Hz	✓	✓
EEGPT2 [27]	✓, 256Hz	✓	✓
MBrain [28]	×	×	×
NeuroLM [29]	✓, 200Hz	✓	✓
CBraMod [30]	✓, 200Hz	✓	✓
EEGFormer [31]	×	×	×

1. - Indicates that the corresponding article does not explicitly mention the size or length of EEG datasets for pre-training.
2. It is worth noting that Brant-2 [20] did not uniformly resample the pre-training data in the resampling, which allowed for brain recordings of varying lengths, sampling rates, and electrode counts, enhancing the flexibility of BrainWave for joint pretraining and deployment on iEEG and EEG data.
3. BIOT [23] conducted Ablation Study on Target Resampling Rate.
4. In Brant-2 [20], BIOT [23], BrainBERT [25], the resampling frequency is different for different tasks.
5. MBrain [28] and EEGFormer [31] do not mention the description of data preprocessing.

### C. Parameter Size

In the pre-training of EEG-FM, the parameter size of the EEG-FM depends on multiple factors, including the model architecture, the number of layers, the number of neurons in each layer, and the dimension of the input data. In this section, we collect the parameter sizes of all large models, see the TabV.

TABLE V: The parameter size of EEG-FMs.

Model	Model type	Size
Brant [19]	Brant	505.69M
Brant-2 [19]	Brant-2	-
LaBraM [21]	LaBraM-Base	5.8M
	LaBraM-Large	46M
	LaBraM-Huge	369M
NeuroGPT [22]	NeuroGPT	79.53M
BIOT [23]	BIOT	3.2M
EEGPT1 [24]	EEGPT-Tiny	4.7M
	EEGPT-Base	25M
BrainBERT [25]	BrainBERT	43.18M
FoME [26]	FoME-Base	476.3M
	FoME-Large	744.8M
EEGPT2 [25]	EEGPT-Base	1.46M
	EEGPT-Large	11.29M
	EEGPT-Huge	183.8M
	EEGPT-Giant	1.09B
MBrain [28]	MBrain	-
	NeuroLM-B	254M
	NeuroLM-L	500M
NeuroLM [29]	NeuroLM-XL	1696M
CBraMod [30]	CBraMod	4.0M
EEGFormer [31]	EEGFormer	-

- Indicates that the corresponding article does not explicitly mention the parameter size of model.

#### D. Downstream Task Types

The performance of large EEG models is mainly evaluated through several types of downstream tasks, which can be divided into the following categories:

- **Classification Tasks:** These include emotion recognition, seizure detection, cognitive state classification, sleep stage identification, and motor imagery recognition.
- **Short-term Prediction:** These tasks involve predicting EEG signal trends or cognitive states over short time horizons.
- **Long-term Prediction:** Long-term prediction tasks focus on forecasting EEG signal patterns or brain state transitions over extended periods. These tasks are essential for applications such as neurodegenerative disease monitoring or long-term cognitive assessment.
- **Imputation:** EEG signal imputation addresses the challenge of missing or corrupted data segments.

At the same time, ablation experiments and model analysis are also essential. This section mainly summarizes the downstream tasks and model evaluation methods selected by these EEG-FMs, see TabVI.

#### E. Self-Supervise Learning

Self-supervised representation learning is a powerful approach to extract high level abstract representation from unlabelled data. Among those methods to learn representation via self-supervised pre-training, masked autoencoder (MAE) has been proved to be a simple but effective way in many fields [13], [16], [32]. After preprocessing all datasets involved in pre-training, we further organize the data into multiple signal blocks with approximately equal data volumes. The model treats each signal block as the minimal input unit. This enables cyclical pre-training on multiple datasets. We begin by segmenting the input signal into patches and randomly replacing a certain percentage (e.g. 40%) of the patches with learnable mask embeddings [MASK]. Then the generalization of the EEG-FM is enhanced by minimizing the reconstruction loss. It should be noted that the reconstruction objectives of different models are different, see the TabVII.

#### F. Hardware for pretraining

In this section we summarize the hardware conditions for the pre-training of EEG-FM, see the Tab.VIII.

### IV. DISCUSSION

#### A. Model Architectures

Approaches such as transformer-based frameworks (e.g., EEGPT and BrainBERT) have demonstrated their efficacy in handling the temporal and spatial complexities of EEG data. For instance, EEGPT’s electrode-wise modeling and hierarchical design allow for independent processing of spatial and temporal features, which is crucial given the high variability and noise inherent in EEG signals. Meanwhile, FoME’s adaptive temporal-lateral attention scaling enhances its ability to model long-range dependencies in EEG recordings. Models

like Brant-2 and LaBraM have integrated multimodal capabilities by leveraging shared representations across invasive and non-invasive signals, further advancing the adaptability and robustness of EEG models.

#### B. Pre-training Strategies and Data Utilization

Pre-training strategies have been pivotal in overcoming the scarcity of labeled EEG data. Self-supervised learning, including masked autoencoding and autoregressive modeling, has emerged as a cornerstone for many EEG foundation models. For example, EEGPT and Brant-2 utilize masked pretraining to learn robust and generalizable representations, enabling effective fine-tuning across downstream tasks. The incorporation of massive datasets, such as those used in LaBraM and Brant, has also contributed significantly to the generalizability of these models. However, these approaches often require meticulous preprocessing and alignment of diverse datasets, which remains a logistical and computational challenge.

#### C. Performance Evaluation

EEG foundation models have been extensively evaluated across a wide range of tasks, including emotion recognition, cognitive state classification, seizure detection, and motor imagery. However, the lack of standardized benchmarks and datasets hinders direct comparisons and may obscure the full capabilities of these models.

#### D. Future Directions

Although great progress has been made in the research of EEG foundation models, several promising directions can still be found in the rapidly developing field of EEG-FM research.

First, almost all current EEG-FMs use a self-supervised learning framework with masks. The key operation to achieve this is to segment the EEG signal into blocks, inspired by block embeddings in images. A comprehensive comparison of the various detailed parameters of EEG segmentation (e.g. the architecture settings of EEG-FM, the sampling rate of the EEG signal, the length of the EEG patches, the overlap rate between the EEG patches, the percentage of data masked in self-supervised training and the selection of pre-training datasets) with respect to their influence on downstream tasks performance should be carried out to address this crucial design question in a systematic manner. Only articles [22], [23] reported the impact of various detailed parameters of EEG segmentation on the experimental results: Article [22] mentioned that increasing the length of patches, increasing the number of patches, reducing the overlapping ratio, increasing the embedding dimension, and increasing the number of self-attention layers in the encoder can enhance the model performance of downstream tasks, the article does not provide convincing data and charts to prove its conclusions. Article [23] mentioned that increasing the length of blocks, the sampling rate of the EEG signal and increasing the overlapping ratio can enhance the model performance of downstream tasks with detailed ablation experiments. However, their views differ in the overlapping ratio.

TABLE VI: The types of downstream tasks

Model	Classification	Short-term Prediction	Long-term Prediction	Imputation	Others
Brant [19]	Seizure detection	✓	✓	✓	Frequency-phase forecasting
Brant-2 [20]	Alzheimer’s disease diagnosis				
	Seizure detection				
	MDD diagnosis				
	Depression diagnosis	×	×	×	-
	Schizophrenia diagnosis				
LaBraM [21]	ADHD diagnosis				
	Sleep deprivation detection				
NeuroGPT [22]	Abnormal detection				
	Event type classification	×	×	×	Regression
BIOT [23]	Emotion recognition				
	Motor Imagery classification	×	×	×	-
	Seizure detection				
	Event type classification				
EEGPT1 [24]	Seizure type classification	×	×	×	-
	Arrhythmias phenotype prediction				
	Huamn action recognition				
	Abnormal detection				
	Event type classification				
BrainBERT [25]	Motor Imagery classification	×	×	×	-
	Sleep stage detection				
	Error related negativity detection				
	Event-related potentials detection				
FoME [26]	Sentence onset				
	Speech vs. non-speech	×	×	×	-
	Volume				
EEGPT2 [27]	Pitch				
	Seizure detection				
	Sleep stage detection	✓	✓	✓	-
	Emotion recognition				
MBrain [28]	Event type classification				
	Emotion Recognition				
	Motor Imagery classification	×	×	×	-
	Mental workload detection				
NeuroLM [29]	Sleeping stage detection				
	Cross Modality				
	Seizure detection	×	×	×	-
	Emotion recognition				
	Abnormal detection				
CBraMod [30]	Event Type Classification				
	Emotion Recognition	×	×	×	-
	Sleep Stage Classification				
	Workload Detection				
	Slowing Event Detection				
	Abnormal detection				
EEGFormer [31]	Event Type Classification	×	×	×	-
	Sleeping Event Detection				
	Seizure Detection				
	Imagined Speech Classification				
EEGFormer [31]	Motor Imagery Classification				
	MDD Diagnosis				
	Abnormal detection				
	Event Type Classification	×	×	×	-
EEGFormer [31]	Sleeping Event Detection				
	Seizure Detection				

1. MDD stands for Major Depressive Disorder.
2. ADHD stands for Attention deficit hyperactivity disorder.

Secondly, GNN can be considered to capture the spatial pattern of EEG signals. We found that EEGPT2 [27] and [103] has tried to integrate GNN into EEG-FM to better capture the potential spatial features of EEG signals. Thirdly, the number of parameters of EEG-FM is still small compared to the current mainstream large language models(e.g. ChatGPT-4o). How to design models that fit specific tasks well but

have small parameters, and how to design models with large parameters and strong generalization will be the focus of future work. Fourthly, designing a model that generates EEG signals from language will be a competitive direction, which may solve the problem of lack of model pre-training EEG signals. Finally, combining EEG models with other modes such as language and imaging to create multimodal vertical

TABLE VII: The reconstruction objectives of EEG-FM

Model	Reconstruction Objective	Loss Function
Brant [19]	Original patches	$\mathcal{L}_{op}$
Brant-2 [20]	Embedded tokens	$\mathcal{L}_{pe}$
LaBraM [21]	Fourier Spectrum prediction	$\mathcal{L}_A + \mathcal{L}_\phi + \mathcal{L}_{nnt} + \mathcal{L}_{eq}$
	Codebook prediction	
NeuroGPT [22]	Embedded tokens	$\mathcal{L}_{pe}$
BIOT [23]	Embedded tokens	$\mathcal{L}_{pe}$
EEGPT1 [24]	Original patches	$\mathcal{L}_{op}$
BrainBERT [25]	Masked spectrogram	$\mathcal{L}_{pe}$
FoME [26]	Original patches	$\mathcal{L}_{op}$
EEGPT2 [27]	Original patches	$\mathcal{L}_{op}$
MBrain [28]	-	-
	Original patches	
NeuroLM [29]	Frequency magnitude	$\mathcal{L}_{op} + \mathcal{L}_\phi + \mathcal{L}_{nnt} + \mathcal{L}_{eq}$
	Codebook prediction	
CBraMod [30]	Original patches	$\mathcal{L}_{op}$
EEGFormer [31]	Original patches	$\mathcal{L}_{op} + \mathcal{L}_{nnt} + \mathcal{L}_{eq}$
	Codebook prediction	

1. - Indicates that the corresponding article does not explicitly mention the reconstruction details of EEG-FM.
2. In LaBraM [21], the loss fails to converge while directly reconstructing raw EEG signals(Original patches).
3. NeuroLM [29] observes that reconstructing the phase contributes minor to neural tokenizer training.

TABLE VIII: The hardware conditions for the pre-training of EEG-FM

Model	GPU	Time	Quantity
Brant [19]	NVIDIA Tesla A100	2.8 days	4
Brant-2 [20]	NVIDIA Tesla A100	100 hours	4
LaBraM [21]	NVIDIA A800	-	-
NeuroGPT [22]	-	-	-
BIOT [23]	NVIDIA RTX A6000	-	8
EEGPT1 [24]	NVIDIA RTX 3090	-	8
BrainBERT [25]	-	-	-
FoME [26]	NVIDIA RTX 4090	350 hours	6
EEGPT2 [27]	NVIDIA A800-SXM4	20 hours	8
MBrain [28]	-	-	-
NeuroLM [29]	NVIDIA Tesla A100	-	8
CBraMod [30]	NVIDIA RTX A5000	5 days	4
EEGFormer [31]	-	-	-

- Indicates that the corresponding article does not explicitly mention the hardware conditions for pre-training.

fields EEG-FM is expected to create an overall framework connecting neuroscience and artificial intelligence, opening up new avenues for research and application.

## V. CONCLUSION

EEG-FMs have become a powerful tool for analyzing and understanding EEG signals. Through their advanced architectures and pre-training strategies, these models have achieved superior performance in various tasks, including disease diagnosis, sleep monitoring, and emotion classification. In this article, we summarize various details of EEG-FMs, including pre-training techniques, pre-training datasets, downstream task datasets, etc. As EEG-based models continue to advance, their transformative impact on healthcare, neuroscience, and brain-computer interface technology is expected to grow, bridging the gap between theoretical progress and practical applications.

In summary, EEG-FMs are expected to improve our understanding of the brain and develop new applications in neuroscience and healthcare. Continued research and innovation

in this field will help develop more accurate, efficient, and interpretable EEG-FM, ultimately achieving better diagnosis, treatment, and rehabilitation of neurological diseases.

## REFERENCES

- [1] Xiang Li, Yazhou Zhang, Prayag Tiwari, Dawei Song, Bin Hu, Meihong Yang, Zhigang Zhao, Neeraj Kumar, and Pekka Martinen. Eeg based emotion recognition: A tutorial and review. *ACM Computing Surveys*, 55(4):1–57, 2022.
- [2] Eunjin Jeon, Wonjun Ko, Jee Seok Yoon, and Heung-Il Suk. Mutual information-driven subject-invariant and class-relevant deep representation learning in bci. *IEEE Transactions on Neural Networks and Learning Systems*, 34(2):739–749, 2021.
- [3] Yang Du, Yongling Xu, Xiaoran Wang, Li Liu, and Pengcheng Ma. Eeg temporal-spatial transformer for person identification. *Scientific Reports*, 12(1):14378, 2022.
- [4] Poomipat Boonyakitantont, Apiwat Lek-Uthai, Krisnachai Chomtho, and Jitkomut Songsiri. A review of feature extraction and performance evaluation in epileptic seizure detection using eeg. *Biomedical Signal Processing and Control*, 57:101702, 2020.
- [5] Lakhyan Dev Sharma, Vijay Kumar Bohat, Maria Habib, Al-Zoubi Ala'M, Hossam Faris, and Ibrahim Aljarah. Evolutionary inspired approach for mental stress detection using eeg signal. *Expert systems with applications*, 197:116634, 2022.
- [6] Khalid Ali I Aboalayon, Miad Faezipour, Wafaa S Almuhammadi, and Saeid Moslehpour. Sleep stage classification using eeg signal analysis: a comprehensive survey and new investigation. *Entropy*, 18(9):272, 2016.
- [7] Syed Umar Amin, Mansour Alsulaiman, Ghulam Muhammad, Mohamed Amine Mekhtiche, and M Shamim Hossain. Deep learning for eeg motor imagery classification based on multi-layer cnns feature fusion. *Future Generation computer systems*, 101:542–554, 2019.
- [8] Subhrajit Roy, Isabell Kiral-Kornek, and Stefan Harrer. Chrononet: A deep recurrent neural network for abnormal eeg identification. In *Artificial Intelligence in Medicine: 17th Conference on Artificial Intelligence in Medicine, AIME 2019, Poznan, Poland, June 26–29, 2019, Proceedings 17*, pages 47–56. Springer, 2019.
- [9] Nazmi Sofian Suhaimi, James Mountstephens, and Jason Teo. Eeg-based emotion recognition: a state-of-the-art review of current trends and opportunities. *Computational intelligence and neuroscience*, 2020(1):8875426, 2020.
- [10] Wouter Biesmans, Neetha Das, Tom Francart, and Alexander Bertrand. Auditory-inspired speech envelope extraction methods for improved eeg-based auditory attention detection in a cocktail party scenario. *IEEE transactions on neural systems and rehabilitation engineering*, 25(5):402–412, 2016.
- [11] Yudhajit Das, Hanli Liu, Fenghua Tian, Srinivas Kota, Rong Zhang, and Lina F Chalak. Rigor of neurovascular coupling (nvc) assessment in newborns using different amplitude eeg algorithms. *Scientific reports*, 10(1):9183, 2020.
- [12] Yiping Wang, Yanfeng Yang, Gongpeng Cao, Jinjie Guo, Penghu Wei, Tao Feng, Yang Dai, Jinguo Huang, Guixia Kang, and Guoguang Zhao. Seeg-net: An explainable and deep learning-based cross-subject pathological activity detection method for drug-resistant epilepsy. *Computers in Biology and Medicine*, 148:105703, 2022.
- [13] Jacob Devlin. Bert: Pre-training of deep bidirectional transformers for language understanding. *arXiv preprint arXiv:1810.04805*, 2018.
- [14] Libo Qin, Qiguang Chen, Xiachong Feng, Yang Wu, Yongheng Zhang, Yinghui Li, Min Li, Wanxiang Che, and Philip S Yu. Large language models meet nlp: A survey. *arXiv preprint arXiv:2405.12819*, 2024.
- [15] Xinlei Chen, Saining Xie, and Kaiming He. An empirical study of training self-supervised vision transformers. In *Proceedings of the IEEE/CVF international conference on computer vision*, pages 9640–9649, 2021.
- [16] Kaiming He, Xinlei Chen, Saining Xie, Yanghao Li, Piotr Dollár, and Ross Girshick. Masked autoencoders are scalable vision learners. In *Proceedings of the IEEE/CVF conference on computer vision and pattern recognition*, pages 16000–16009, 2022.
- [17] Raby Hamadi. Large language models meet computer vision: A brief survey. *arXiv preprint arXiv:2311.16673*, 2023.
- [18] Jonathan W Kim, Ahmed Alaa, and Danilo Bernardo. Eeg-gpt: exploring capabilities of large language models for eeg classification and interpretation. *arXiv preprint arXiv:2401.18006*, 2024.

- [19] Daoze Zhang, Zhizhang Yuan, Yang Yang, Junru Chen, Jingjing Wang, and Yafeng Li. Brant: Foundation model for intracranial neural signal. *Advances in Neural Information Processing Systems*, 36, 2024.
- [20] Zhizhang Yuan, Daoze Zhang, Junru Chen, Geifei Gu, and Yang Yang. Brant-2: Foundation model for brain signals. *arXiv preprint arXiv:2402.10251*, 2024.
- [21] Wei-Bang Jiang, Li-Ming Zhao, and Bao-Liang Lu. Large brain model for learning generic representations with tremendous eeg data in bci. *arXiv preprint arXiv:2405.18765*, 2024.
- [22] Wenhui Cui, Woojae Jeong, Philipp Thölke, Takfarinas Medani, Karim Jerbi, Anand A Joshi, and Richard M Leahy. Neuro-gpt: Towards a foundation model for eeg. In *2024 IEEE International Symposium on Biomedical Imaging (ISBI)*, pages 1–5. IEEE, 2024.
- [23] C Yang, MB Westover, and J Sun. Biot: Cross-data biosignal learning in the wild [internet]. arxiv: 2023 [cited 2023 may 30].
- [24] Guangyu Wang, Wencao Liu, Yuhong He, Cong Xu, Lin Ma, and Haifeng Li. Eegpt: Pretrained transformer for universal and reliable representation of eeg signals. In *The Thirty-eighth Annual Conference on Neural Information Processing Systems*, 2024.
- [25] Christopher Wang, Vighnesh Subramaniam, Adam Uri Yaari, Gabriel Kreiman, Boris Katz, Ignacio Cases, and Andrei Barbu. Brainbert: Self-supervised representation learning for intracranial recordings. *arXiv preprint arXiv:2302.14367*, 2023.
- [26] Enze Shi, Kui Zhao, Qilong Yuan, Jiaqi Wang, Huawen Hu, Sigang Yu, and Shu Zhang. Fome: A foundation model for eeg using adaptive temporal-lateral attention scaling. *arXiv preprint arXiv:2409.12454*, 2024.
- [27] Tongtian Yue, Shuning Xue, Xuange Gao, Yepeng Tang, Longteng Guo, Jie Jiang, and Jing Liu. Eegpt: Unleashing the potential of eeg generalist foundation model by autoregressive pre-training. *arXiv preprint arXiv:2410.19779*, 2024.
- [28] Donghong Cai, Junru Chen, Yang Yang, Teng Liu, and Yafeng Li. Mbrain: A multi-channel self-supervised learning framework for brain signals. In *Proceedings of the 29th ACM SIGKDD Conference on Knowledge Discovery and Data Mining*, pages 130–141, 2023.
- [29] Wei-Bang Jiang, Yansen Wang, Bao-Liang Lu, and Dongsheng Li. Neurolm: A universal multi-task foundation model for bridging the gap between language and eeg signals. *arXiv preprint arXiv:2409.00101*, 2024.
- [30] Jiquan Wang, Sha Zhao, Zhiling Luo, Yangxuan Zhou, Haiteng Jiang, Shijian Li, Tao Li, and Gang Pan. Cbramod: A criss-cross brain foundation model for eeg decoding. *arXiv preprint arXiv:2412.07236*, 2024.
- [31] Yuqi Chen, Kan Ren, Kaitao Song, Yansen Wang, Yifan Wang, Dongsheng Li, and Lili Qiu. Eegformer: Towards transferable and interpretable large-scale eeg foundation model. *arXiv preprint arXiv:2401.10278*, 2024.
- [32] Yuqi Nie, Nam H Nguyen, Phanwadee Sinthong, and Jayant Kalagnanam. A time series is worth 64 words: Long-term forecasting with transformers. *arXiv preprint arXiv:2211.14730*, 2022.
- [33] HJ Landau. Sampling, data transmission, and the nyquist rate. *Proceedings of the IEEE*, 55(10):1701–1706, 1967.
- [34] Ronald N Bracewell. The fourier transform. *Scientific American*, 260(6):86–95, 1989.
- [35] Zhiliang Peng, Li Dong, Hangbo Bao, Qixiang Ye, and Furu Wei. Beit v2: Masked image modeling with vector-quantized visual tokenizers. *arXiv preprint arXiv:2208.06366*, 2022.
- [36] Petr Nejedly, Vaclav Kremen, Vladimir Sladky, Jan Cimbalnik, Petr Klimes, Filip Plesinger, Filip Mivalt, Vojtech Travnicek, Ivo Viscor, Martin Pail, et al. Multicenter intracranial eeg dataset for classification of graphoelements and artifactual signals. *Scientific data*, 7(1):179, 2020.
- [37] Dorien van Blooijis, Max A van den Boom, Jaap F van der Aar, Geert-Jan M Huiskamp, Giulio Castegnar, Matteo Demuru, Willemiek JEM Zweiphenning, Pieter van Eijsden, Kai J Miller, Frans SS Leijten, et al. Developmental trajectory of transmission speed in the human brain. *Nature Neuroscience*, 26(4):537–541, 2023.
- [38] Andreas Miltiadous, Katerina D Tzamoura, Theodora Afrantou, Panagiotis Ioannidis, Nikolaos Grigoriadis, Dimitrios G Tsalikakis, Pantelis Angelidis, Markos G Tsipouras, Evripidis Glavas, Nikolaos Gianakeas, et al. A dataset of eeg recordings from: Alzheimer’s disease, frontotemporal dementia and healthy subjects. *OpenNeuro*, 1:88, 2023.
- [39] Mario Giovanni Terzano, Liborio Parrino, Arianna Smerieri, Ronald Chervin, Sudhansu Chokroverty, Christian Guillemainault, Max Hirschkowitz, Mark Mahowald, Harvey Moldofsky, Agostino Rosa, et al. Atlas, rules, and recording techniques for the scoring of cyclic alternating pattern (cap) in human sleep. *Sleep medicine*, 3(2):187–199, 2002.
- [40] J. Guttg. Chb-mit scalp eeg database (version 1.0.0). <https://doi.org/10.13026/C2K01R>, 2010. PhysioNet.
- [41] Diego Alvarez-Estevéz and Roselyne M Rijsman. Inter-database validation of a deep learning approach for automatic sleep scoring. *PLoS one*, 16(8):e0256111, 2021.
- [42] Paolo Detti, Giampaolo Vatti, and Garazi Zabalo Manrique de Lara. Eeg synchronization analysis for seizure prediction: A study on data of noninvasive recordings. *Processes*, 8(7):846, 2020.
- [43] Christoffer Hatlestad-Hall, Trine Waage Rygvold, and Stein Andersson. Bids-structured resting-state electroencephalography (eeg) data extracted from an experimental paradigm. *Data in Brief*, 45:108647, 2022.
- [44] Wajid Mumtaz. Mdd patients and healthy controls eeg data (new). *Figshare, Dataset*, 2016.
- [45] Amir Harati, Silvia Lopez, I Obeid, J Picone, MP Jacobson, and S Tobochnik. The tuh eeg corpus: A big data resource for automated eeg interpretation. In *2014 IEEE signal processing in medicine and biology symposium (SPMB)*, pages 1–5. IEEE, 2014.
- [46] OpenNeuro. ds003478: [dataset title]. <https://openneuro.org/datasets/ds003478/versions/1.1.0>, 2021. Version 1.1.0.
- [47] Elzbieta Olejarczyk and Wojciech Jernajczyk. EEG in schizophrenia, 2017.
- [48] Bob Kemp, Aeilko H Zwinderman, Bert Tuk, Hilbert AC Kamphuisen, and Josefien JL Obery. Analysis of a sleep-dependent neuronal feedback loop: the slow-wave microcontinuity of the eeg. *IEEE Transactions on Biomedical Engineering*, 47(9):1185–1194, 2000.
- [49] Ghasem Sadeghi Bajestani, Shima Abedian, Fatemeh Makhlooghi, Motahhareh Raoufitabar, and Hamid Saeedi. A dataset of eeg signals from adults with adhd and healthy controls: Resting state, cognitive function, and sound listening paradigm. <https://doi.org/10.17632/6k4g25fhzg.1>, 2023. Mendeley Data, V1.
- [50] Haijie Liu and Xiaodong Lv. EEG datasets of stroke patients. 12 2022.
- [51] Ali Motie Nasrabadi, Armin Allahverdy, Mehdi Samavati, and Mohammad Reza Mohammadi. Eeg data for adhd / control children, 2020.
- [52] AP Rockhill, N Jackson, JS George, AR Aron, and NC Swann. Uc san diego resting state eeg data from patients with parkinson’s disease. openneuro [dataset], 2021.
- [53] Chuqin Xiang, Xinrui Fan, Duo Bai, Ke Lv, and Xu Lei. A resting-state eeg dataset for sleep deprivation. *Scientific Data*, 11(1):427, 2024.
- [54] Mário L Vicchietti, Fernando M Ramos, Luiz E Betting, and Andriana SLO Campanharo. Computational methods of eeg signals analysis for alzheimer’s disease classification. *Scientific Reports*, 13(1):8184, 2023.
- [55] Benjamin Blankertz, Guido Dornhege, Matthias Krauledat, Klaus-Robert Müller, and Gabriel Curio. The non-invasive berlin brain-computer interface: fast acquisition of effective performance in untrained subjects. *NeuroImage*, 37(2):539–550, 2007.
- [56] Iyad Obeid and Joseph Picone. The temple university hospital eeg data corpus. *Frontiers in neuroscience*, 10:196, 2016.
- [57] Arman Savran, Koray Ciftci, Guillaume Chanel, Javier Cruz\_Mota, Luong Hong Viet, Bülent Sankur, Lale Akarun, Alice Caplier, and Michele Rombaut. Emotion detection in the loop from brain signals and facial images. In *eINTERFACE’06-SIMILAR NoE Summer Workshop on Multimodal Interfaces*, 2006.
- [58] Matthew D Luciw, Ewa Jarocka, and Benoni B Edin. Multi-channel eeg recordings during 3,936 grasp and lift trials with varying weight and friction. *Scientific data*, 1(1):1–11, 2014.
- [59] Wei Liu, Jie-Lin Qiu, Wei-Long Zheng, and Bao-Liang Lu. Comparing recognition performance and robustness of multimodal deep learning models for multimodal emotion recognition. *IEEE Transactions on Cognitive and Developmental Systems*, 14(2):715–729, 2021.
- [60] Perrin Margaux, Maby Emmanuel, Daligault Sébastien, Bertrand Olivier, and Mattout Jérémie. Objective and subjective evaluation of online error correction during p300-based spelling. *Advances in Human-Computer Interaction*, 2012(1):578295, 2012.
- [61] Yongtian He, Trieu Phat Luu, Kevin Nathan, Sho Nakagome, and Jose L Contreras-Vidal. A mobile brain-body imaging dataset recorded during treadmill walking with a brain-computer interface. *Scientific data*, 5(1):1–10, 2018.
- [62] Gerwin Schalk, Dennis J McFarland, Thilo Hinterberger, Niels Birbaumer, and Jonathan R Wolpaw. Bci2000: a general-purpose brain-computer interface (bci) system. *IEEE Transactions on biomedical engineering*, 51(6):1034–1043, 2004.

- [63] Texas Data Repository. Dataset title. <https://dataverse.tdl.org/dataset.xhtml?persistentId=doi:10.18738/T8/SS2NHB>, 2020. Accessed via Texas Data Repository.
- [64] Logan T Trujillo, Candice T Stanfield, and Ruben D Vela. The effect of electroencephalogram (eeg) reference choice on information-theoretic measures of the complexity and integration of eeg signals. *Frontiers in neuroscience*, 11:425, 2017.
- [65] Louis Korczowski, Martine Cederhout, Anton Andreev, Grégoire Cattan, Pedro Luiz Coelho Rodrigues, Violette Gautheret, and Marco Congedo. *Brain Invaders calibration-less P300-based BCI with modulation of flash duration Dataset (bi2015a)*. PhD thesis, GIPSA-lab, 2019.
- [66] G Buckwalter, S Chhin, S Rahman, I Obeid, and J Picone. Recent advances in the tuh eeg corpus: improving the interrater agreement for artifacts and epileptiform events. In *2021 IEEE Signal Processing in Medicine and Biology Symposium (SPMB)*, pages 1–3. IEEE, 2021.
- [67] L Veloso, J McHugh, E Von Weltin, S Lopez, I Obeid, and J Picone. Big data resources for eegs: Enabling deep learning research. In *2017 IEEE Signal Processing in Medicine and Biology Symposium (SPMB)*, pages 1–3. IEEE, 2017.
- [68] Eva von Weltin, Tameem Ahsan, Vinit Shah, Dawer Jamshed, Meysam Golmohammadi, Iyad Obeid, and Joseph Picone. Electroencephalographic slowing: A primary source of error in automatic seizure detection. In *2017 IEEE Signal Processing in Medicine and Biology Symposium (SPMB)*, pages 1–5. IEEE, 2017.
- [69] Wei-Long Zheng and Bao-Liang Lu. Investigating critical frequency bands and channels for eeg-based emotion recognition with deep neural networks. *IEEE Transactions on autonomous mental development*, 7(3):162–175, 2015.
- [70] Wei-Long Zheng, Wei Liu, Yifei Lu, Bao-Liang Lu, and Andrzej Cichocki. Emotionmeter: A multimodal framework for recognizing human emotions. *IEEE transactions on cybernetics*, 49(3):1110–1122, 2018.
- [71] Wei-Bang Jiang, Xuan-Hao Liu, Wei-Long Zheng, and Bao-Liang Lu. Multimodal adaptive emotion transformer with flexible modality inputs on a novel dataset with continuous labels. In *Proceedings of the 31st ACM International Conference on Multimedia*, pages 5975–5984, 2023.
- [72] Wei-Bang Jiang, Li-Ming Zhao, Ping Guo, and Bao-Liang Lu. Discriminating surprise and anger from eeg and eye movements with a graph network. In *2021 IEEE International Conference on Bioinformatics and Biomedicine (BIBM)*, pages 1353–1357. IEEE, 2021.
- [73] Shuai Luo, Yu-Ting Lan, Dan Peng, Ziyi Li, Wei-Long Zheng, and Bao-Liang Lu. Multimodal emotion recognition in response to oil paintings. In *2022 44th Annual International Conference of the IEEE Engineering in Medicine & Biology Society (EMBC)*, pages 4167–4170. IEEE, 2022.
- [74] Rui Li, Le-Dian Liu, and Bao-Liang Lu. Discrimination of decision confidence levels from eeg signals. In *2021 10th International IEEE/EMBS Conference on Neural Engineering (NER)*, pages 946–949. IEEE, 2021.
- [75] Le-Yan Tao and Bao-Liang Lu. Emotion recognition under sleep deprivation using a multimodal residual lstm network. In *2020 International Joint Conference on Neural Networks (IJCNN)*, pages 1–8. IEEE, 2020.
- [76] Michael Tangermann, Klaus-Robert Müller, Ad Aertsen, Niels Birbaumer, Christoph Braun, Clemens Brunner, Robert Leeb, Carsten Mehring, Kai J Miller, Gernot R Müller-Putz, et al. Review of the bci competition iv. *Frontiers in neuroscience*, 6:55, 2012.
- [77] Guo-Qiang Zhang, Licong Cui, Remo Mueller, Shiqiang Tao, Matthew Kim, Michael Rueschman, Sara Mariani, Daniel Mobley, and Susan Redline. The national sleep research resource: towards a sleep data commons. *Journal of the American Medical Informatics Association*, 25(10):1351–1358, 2018.
- [78] Stuart F Quan, Barbara V Howard, Conrad Iber, James P Kiley, F Javier Nieto, George T O'Connor, David M Rapoport, Susan Redline, John Robbins, Jonathan M Samet, et al. The sleep heart health study: design, rationale, and methods. *Sleep*, 20(12):1077–1085, 1997.
- [79] Erick A Perez Alday, Annie Gu, Amit J Shah, Chad Robichaux, An-Kwok Ian Wong, Chengyu Liu, Feifei Liu, Ali Bahrami Rad, Andoni Elola, Salman Seyedi, et al. Classification of 12-lead eegs: the physionet/computing in cardiology challenge 2020. *Physiological measurement*, 41(12):124003, 2020.
- [80] Wendong Ge, Jin Jing, Sungtae An, Aline Herlopian, Marcus Ng, Aaron F Struck, Brian Appavu, Emily L Johnson, Gamaleldin Osman, Hiba A Haider, et al. Deep active learning for interictal ictal injury continuum eeg patterns. *Journal of neuroscience methods*, 351:108966, 2021.
- [81] Patrick Wagner, Nils Strothoff, Ralf-Dieter Boussejot, Dieter Kreiseler, Fatima I Lunze, Wojciech Samek, and Tobias Schaeffter. Ptb-xl, a large publicly available electrocardiography dataset. *Scientific data*, 7(1):1–15, 2020.
- [82] Davide Anguita, Alessandro Ghio, Luca Oneto, Xavier Parra, Jorge Luis Reyes-Ortiz, et al. A public domain dataset for human activity recognition using smartphones. In *Esann*, volume 3, page 3, 2013.
- [83] Ary L Goldberger, Luis AN Amaral, Leon Glass, Jeffrey M Hausdorff, Plamen Ch Ivanov, Roger G Mark, Joseph E Mietus, George B Moody, Chung-Kang Peng, and H Eugene Stanley. Physiobank, physiotoolkit, and physionet: components of a new research resource for complex physiologic signals. *circulation*, 101(23):e215–e220, 2000.
- [84] Robin Tibor Schirrmeyer, Jost Tobias Springenberg, Lukas Dominique Josef Fiederer, Martin Glasstetter, Katharina Eggensperger, Michael Tangermann, Frank Hutter, Wolfram Burgard, and Tonio Ball. Deep learning with convolutional neural networks for eeg decoding and visualization. *Human brain mapping*, 38(11):5391–5420, 2017.
- [85] David Steyrl, Reinhold Scherer, Josef Fallner, and Gernot R Müller-Putz. Random forests in non-invasive sensorimotor rhythm brain-computer interfaces: a practical and convenient non-linear classifier. *Biomedical Engineering/Biomedizinische Technik*, 61(1):77–86, 2016.
- [86] Yijun Wang, Xiaogang Chen, Xiaorong Gao, and Shangkai Gao. A benchmark dataset for ssvep-based brain-computer interfaces. *IEEE Transactions on Neural Systems and Rehabilitation Engineering*, 25(10):1746–1752, 2016.
- [87] Gan Huang, Zhenxing Hu, Weize Chen, Shaorong Zhang, Zhen Liang, Linling Li, Li Zhang, and Zhiguo Zhang. M3cv: A multi-subject, multi-session, and multi-task database for eeg-based biometrics challenge. *NeuroImage*, 264:119666, 2022.
- [88] Jingjing Chen, Xiaobin Wang, Chen Huang, Xin Hu, Xinke Shen, and Dan Zhang. A large finer-grained affective computing eeg dataset. *Scientific Data*, 10(1):740, 2023.
- [89] Sander Koelstra, Christian Muhl, Mohammad Soleymani, Jong-Seok Lee, Ashkan Yazdani, Touradj Ebrahimi, Thierry Pun, Anton Nijholt, and Ioannis Patras. Deap: A database for emotion analysis; using physiological signals. *IEEE transactions on affective computing*, 3(1):18–31, 2011.
- [90] Wei Liu, Wei-Long Zheng, Ziyi Li, Si-Yuan Wu, Lu Gan, and Bao-Liang Lu. Identifying similarities and differences in emotion recognition with eeg and eye movements among chinese, german, and french people. *Journal of Neural Engineering*, 19(2):026012, 2022.
- [91] Hohyun Cho, Minkyu Ahn, Sangtae Ahn, Moonyoung Kwon, and Sung Chan Jun. Eeg datasets for motor imagery brain-computer interface. *GigaScience*, 6(7):gix034, 2017.
- [92] Tijn Grootswagers, Ivy Zhou, Amanda K Robinson, Martin N Hebart, and Thomas A Carlson. Human eeg recordings for 1,854 concepts presented in rapid serial visual presentation streams. *Scientific Data*, 9(1):3, 2022.
- [93] Igor Zyma, Sergii Tukaev, Ivan Seleznev, Ken Kiyono, Anton Popov, Mariia Chernykh, and Oleksii Shpenkov. Electroencephalograms during mental arithmetic task performance. *Data*, 4(1):14, 2019.
- [94] Alessandro T Gifford, Kshitij Dwivedi, Gemma Roig, and Radoslaw M Cichy. A large and rich eeg dataset for modeling human visual object recognition. *NeuroImage*, 264:119754, 2022.
- [95] Diego Alvarez-Estevéz and RM Rijsman. Haaglanden medisch centrum sleep staging database (version 1.0. 1). *PhysioNet*, 2021.
- [96] Chuong H Nguyen, George K Karavas, and Panagiotis Artemiadis. Inferring imagined speech using eeg signals: a new approach using riemannian manifold features. *Journal of neural engineering*, 15(1):016002, 2017.
- [97] Stamos Katsigiannis and Naeem Ramzan. Dreamer: A database for emotion recognition through eeg and ecg signals from wireless low-cost off-the-shelf devices. *IEEE journal of biomedical and health informatics*, 22(1):98–107, 2017.
- [98] Mastaneh Torkamani-Azar, Sumeyra Demir Kanik, Serap Aydin, and Mujdat Cetin. Prediction of reaction time and vigilance variability from spatio-spectral features of resting-state eeg in a long sustained attention task. *IEEE journal of biomedical and health informatics*, 24(9):2550–2558, 2020.
- [99] Sirvan Khalighi, Teresa Sousa, José Moutinho Santos, and Urbano Nunes. Isruc-sleep: A comprehensive public dataset for sleep researchers. *Computer methods and programs in biomedicine*, 124:180–192, 2016.
- [100] Ji-Hoon Jeong, Jeong-Hyun Cho, Young-Eun Lee, Seo-Hyun Lee, Gi-Hwan Shin, Young-Seok Kweon, José del R Millán, Klaus-Robert Müller, and Seong-Whan Lee. 2020 international brain-computer

- interface competition: A review. *Frontiers in Human Neuroscience*, 16:898300, 2022.
- [101] Jianliang Min, Ping Wang, and Jianfeng Hu. Driver fatigue detection through multiple entropy fusion analysis in an eeg-based system. *PLoS one*, 12(12):e0188756, 2017.
- [102] Nathan J Stevenson, Karoliina Tapani, Leena Lauronen, and Sampsa Vanhatalo. A dataset of neonatal eeg recordings with seizure annotations. *Scientific data*, 6(1):1–8, 2019.
- [103] Limin Wang, Toyotaro Suzumura, and Hiroki Kanezashi. Graph-enhanced eeg foundation model. *arXiv preprint arXiv:2411.19507*, 2024.